

# 1 **Measurements of open heavy-flavor hadrons in Au+Au** 2 **collisions at $\sqrt{s_{NN}} = 200$ GeV by the STAR experiment**

---

3 **Lukáš Kramárik, for the STAR collaboration\***

4 *Department of Physics*

5 *Faculty of Nuclear Sciences and Physical Engineering*

6 *Czech Technical University in Prague*

7 *Břehová 7, 115 19 Prague 1, Czech Republic*

8 *E-mail: [lukas.kramarik@fjfi.cvut.cz](mailto:lukas.kramarik@fjfi.cvut.cz)*

At RHIC energies, heavy-flavor quarks are primarily produced in hard partonic scatterings at early stages of ultra-relativistic heavy-ion collisions. This makes them an excellent probe of the quark-gluon plasma (QGP) since they experience the whole evolution of the hot and dense medium. STAR is able to study the production of charm quarks and their interaction with the QGP through direct reconstruction of hadronic decays of open charm hadrons and the topological separation of electrons originating from bottom and charm hadron decays. This is possible thanks to the excellent track pointing resolution provided by the Heavy Flavor Tracker.

9 In these proceedings, the most recent results on open heavy-flavor hadron production in Au+Au collisions at  $\sqrt{s_{NN}} = 200$  GeV from the STAR experiment are shown. In particular, we will discuss the nuclear modification factor of  $D^0$  meson,  $D_s/D^0$  and  $\Lambda_c^\pm/D^0$  yield ratios as functions of transverse momentum and collision centrality. Additionally, charm and bottom decayed electrons elliptic flow  $v_2$  are presented. Finally, rapidity-dependent directed flow  $v_1$  of  $D^0$  meson and charm decayed electrons are reported.

*40th International Conference on High Energy physics - ICHEP2020  
July 28 - August 6, 2020  
Prague, Czech Republic (virtual meeting)*

---

\*Speaker

## 1. Introduction

Quark-gluon plasma (QGP) is the hot and dense nuclear matter of deconfined quarks and gluons that could be created in ultrarelativistic collisions of heavy ions [1]. Heavy-flavor (HF, charm and bottom) quarks are produced primarily at the early stages of collisions [2] and thus experience the entire evolution of the medium. Directed flow of HF mesons allow us to study initial conditions of heavy-ion collisions, such as the tilt of the QGP medium and the initial electromagnetic (EM) field. Furthermore, collective behavior of HF quarks, reflected in the elliptic flow of HF mesons, is sensitive to the degree of the HF quark thermalization in the QGP and helps constrain the HF quark diffusion coefficient. Study of open-charm meson yields probes not only the quark mass dependence of energy loss in the QGP, but also its hadronization in the heavy-ion collisions.

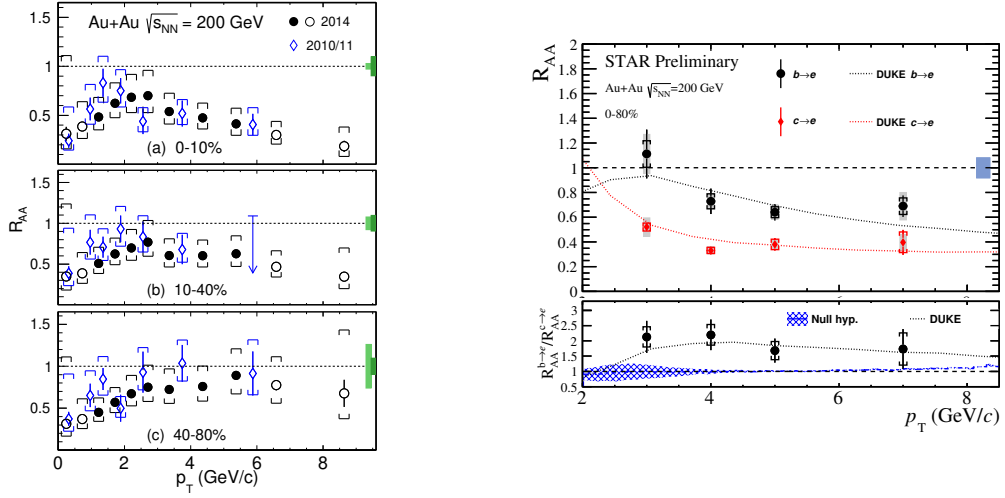
The STAR experiment at the Relativistic Heavy Ion Collider (RHIC) performed extensive studies of the HF hadron production. Results from Au+Au collisions at  $\sqrt{s_{NN}} = 200$  GeV presented in these proceedings are achieved, thanks mainly to the Heavy Flavor Tracker (HFT) [3], the high-precision silicon vertex detector installed at the center of the STAR for data taking in years 2014–2016. It greatly improves the track pointing resolution and enables the topological reconstruction of the secondary vertices of open charm hadron decays through the hadronic channels, such as  $D^0 \rightarrow K^- \pi^+$ ,  $\Lambda_c^+ \rightarrow K^- \pi^+ p$  or  $D_s \rightarrow \phi \pi^+ \rightarrow K^- K^+ \pi^+$ . In addition, the HFT enables the measurement of electrons from charm and bottom hadron decays with great precision. HF decayed electron fractions are extracted using template fits to distributions of the 3D distance of closest approach of a track to the collision vertex.

## 2. Heavy-flavor production in Au+Au collisions

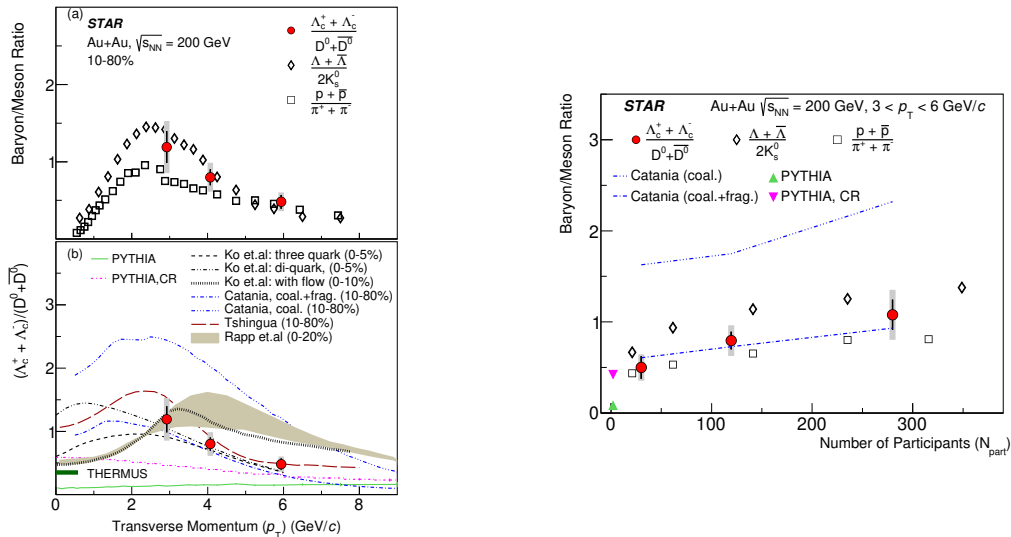
Particle production in Au+Au collisions can be studied using the nuclear modification factor  $R_{AA}$ , defined as the ratio of the invariant particle yields measured in Au+Au and p+p collisions (where no QGP is expected to be created), scaled by the average number of binary nucleon-nucleon collisions in the investigated Au+Au collision centrality interval.  $D^0$  meson  $R_{AA}$  measured in three collision centrality intervals is shown in Fig. 1 (left) [4]. At high transverse momentum,  $p_T$ , yields are greatly suppressed in central collisions, indicating that charm quarks lose a significant amount of energy in the QGP. Towards more peripheral collisions, this suppression at high  $p_T$  decreases. However, at low  $p_T$ ,  $R_{AA}$  has no significant centrality dependence.

Figure 1 (right) shows charm and bottom decayed electron  $R_{AA}$ . Data are consistent with the DUKE model prediction [5] which contains the mass dependence of energy loss. Furthermore, bottom decayed electron suppression is smaller than that of charm decayed electron with a significance larger than  $3\sigma$ . This suggests a quark mass dependence of the energy loss in the QGP.

In order to understand hadronization of the charm quarks,  $\Lambda_c/D^0$  yield ratio is measured [6] and results are shown in Fig. 2. In Fig. 2 (left), it can be seen that in the measured  $p_T$  interval,  $\Lambda_c/D^0$  is comparable to the baryon-to-meson ratios of strange and light flavor hadrons. Additionally, the data are compared to model calculations including different charm quark hadronization mechanisms and QGP medium properties. Both data and calculations that include coalescence hadronization of charm quarks show significant enhancements compared to the PYTHIA calculation. In Fig. 2 (right), centrality dependence of  $\Lambda_c/D^0$  yield ratio shows a similar trend as for light flavor and strange hadron



**Figure 1:** Left: The  $R_{AA}$  of  $D^0$  meson as a function of  $p_T$  in different centrality classes measured with (2014) and without (2010/11) the HFT detector installed. Taken from Ref. [4]. Right: The  $R_{AA}$  of charm and bottom decayed electron (top) and their ratio (bottom), compared to the DUKE model prediction [5].



**Figure 2:** Left:  $\Lambda_c^\pm/D^0$  yield ratio as a function of  $p_T$  compared to light-hadron results (top) and different model calculations (bottom). Right:  $\Lambda_c^\pm/D^0$  yield ratio vs number of participants  $N_{part}$ , compared to light-hadron results, PYTHIA calculation with and without color reconnection and the Catania model incorporating coalescence and fragmentation hadronization of the charm quarks. Taken from Ref. [6].

50 yield ratios. The data are consistent with the Catania model calculation incorporating coalescence  
 51 and fragmentation hadronization of the charm quarks [7].

52 STAR also measured  $D_s/D^0$  yield ratio, that probes both strangeness enhancement and coalescence  
 53 of charm quarks with strange quarks in the QGP. Figure 3 (left top) shows that this ratio  
 54 has no significant centrality dependence and is significantly larger than the fragmentation baseline,  
 55 represented by a PYTHIA8 calculation. In Fig. 3 (left bottom), STAR results in central Au+Au

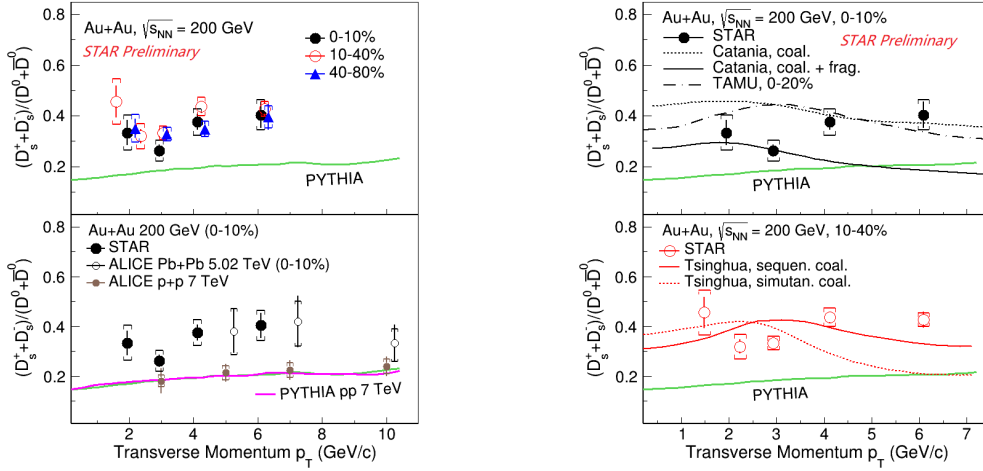


**Figure 3:**  $D_s/D^0$  yield ratio as a function of  $p_T$  in different centralities of Au+Au collisions compared to PYTHIA p+p calculations and to an ALICE measurement [8, 9] (left) and to various models incorporating coalescence and fragmentation hadronization of charm quarks [7, 10, 11] (right).

56 collisions are compared to the ALICE result in central Pb+Pb collisions at  $\sqrt{s_{NN}} = 5.02$  TeV.  
 57 Results are consistent in the overlapping region. Additionally, ALICE p+p data at  $\sqrt{s} = 7$  TeV are  
 58 consistent with a PYTHIA calculation at the same energy.

59 Figure 3 (right) shows comparison of the STAR results in central (right top) and semi-central  
 60 collisions (right bottom) with model calculations. The Catania model calculation with only coales-  
 61 cence hadronization describes data for  $p_T > 4$  GeV/c, however the Catania model calculation with  
 62 both coalescence and fragmentation hadronization describes data for lower  $p_T$ . Furthermore, the  
 63 Tsinghua model with sequential coalescence hadronization of charm quarks qualitatively describes  
 64 data in 10–40% semi-central collisions.

### 65 3. Anisotropic flow of heavy-flavor decayed electrons

66 To quantify the transport properties of the hot medium produced in heavy-ion collisions, col-  
 67 lective behavior of partons is studied via measurement of elliptic flow  $v_2$  of produced particles [12].  
 68 This is the second coefficient of the Fourier decomposition of the azimuthal distribution of the  
 69 particle yield with respect to the event plane. The  $D^0$  meson  $v_2$  measured by STAR in Au+Au  
 70 collisions was found to follow number of constituent quark scaling [13].

71 Figure 4 shows the HF decayed electron  $v_2$ . In this analysis, non-flow effects are calculated using  
 72 electron-hadron correlations in semileptonic charm and bottom decays simulated with PYTHIA.  
 73 Charm decayed electron  $v_2$ , shown in Fig. 4 (left) is consistent with the  $D^0$   $v_2$  [13] folded to  
 74 the decayed electron and the Duke model [5]. For bottom decayed electron  $v_2$ , shown in Fig. 4  
 75 (right), two approaches for the event plane reconstruction are compared. One of them uses tracks  
 76 reconstructed in the Time Projection Chamber (TPC) in the pseudorapidity range of  $|\eta| < 1$ , the latter  
 77 one uses hits in the Forward Meson Spectrometer (FMS) in  $-2.5 < \eta < 4$ . The TPC event plane  
 78 measurement with non-flow subtraction results in non-zero  $v_2$  of bottom decayed electrons with a  
 79 significance of  $3.4\sigma$ . As can be seen, using FMS significantly reduces the non-flow contribution to

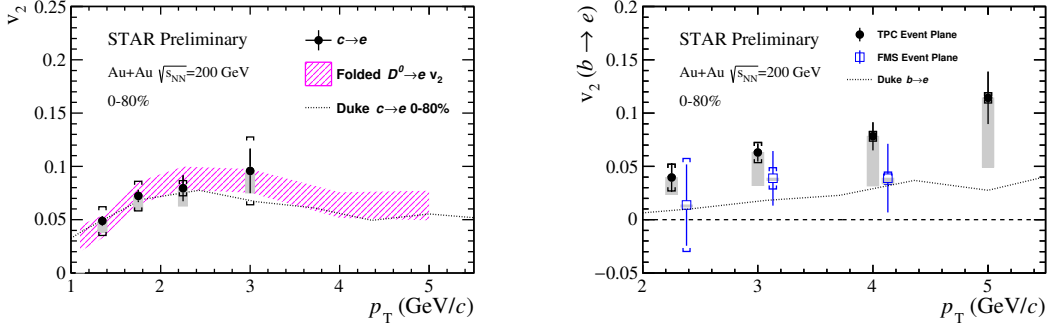


**Figure 4:** Elliptic flow  $v_2$  of charm decayed (left) and bottom decayed electrons (right) as a function of  $p_T$ , compared to folded  $D^0$  meson  $v_2$  [13] and DUKE model calculations [5]. Gray boxes show the estimated non-flow contributions.

80 0.5%. However, this measurement has poorer event-plane resolution and smaller statistics due to  
 81 the FMS being present only in part of the data recorded.

82 Initial conditions of heavy-ion collisions could be accessed via measurement of directed flow,  
 83  $v_1$ , whose magnitude is affected by the initial tilt of the QGP bulk and viscous drag on charm  
 84 quarks. Furthermore, the initial EM field is predicted to induce larger  $v_1$  for charm quarks than for  
 85 light flavor quarks due to the early production of charm quarks and gives opposite contributions to  
 86 charm and anti-charm quarks.

87 Figure 5 (left) shows  $v_1$  of combined  $D^0$  and  $\overline{D}^0$  (top) and difference between  $D^0$  and  $\overline{D}^0$   $v_1$   
 88 (bottom) [14]. Separate measurement of  $D^0$  and  $\overline{D}^0$  is done via topological reconstruction of decays  
 89  $D^0 \rightarrow K^- \pi^+$  and  $\overline{D}^0 \rightarrow K^+ \pi^-$ . The absolute value of the  $D^0$   $v_1$  is observed to be about 25 times larger  
 90 than that of the kaons with a  $3.4\sigma$  significance. Model calculations with a tilted source predict the  
 91 correct sign of  $dv_1/dy$ , but the  $v_1$  magnitudes are lower than data. Study of the initial EM field  
 92 induced splitting for charm decayed electrons is shown in Fig. 5 (right). The  $v_1$  for charm and  
 93 anti-charm is accessed by separate measurements of charm decayed  $e^+$  and anti-charm decayed  $e^-$ .  
 94 Within the uncertainties, no splitting due to EM field is observed in both measurements.

#### 95 4. Summary

96 The STAR experiment, thanks to the HFT detector, measured open heavy-flavor production  
 97 in Au+Au collisions at  $\sqrt{s_{NN}} = 200$  GeV via topological reconstruction of charmed hadrons and  
 98 extraction of HF decayed electrons. Results on the open-charm hadron production suggest that charm  
 99 quarks participate in coalescence hadronization in the QGP and strongly interact with the created  
 100 medium. Additionally, measurements of HF decayed electrons suggest quark mass dependence of  
 101 parton energy loss in the QGP.

102 Charm decayed electron  $v_2$ , consistent with  $D^0$   $v_2$ , indicate that charm quarks gain significant  
 103 flow in the QGP. Firstly observed non-zero bottom decayed electron  $v_2$  is consistent with the Duke  
 104 model incorporating bottom quark transport in the QGP. Predicted charm and anti-charm splitting  
 105 due to the initial EM field is not observed in measured  $v_1$  of  $D^0$  and  $\overline{D}^0$ , as well as charm (anti-charm)  
 106 decayed  $e^+$  ( $e^-$ ).

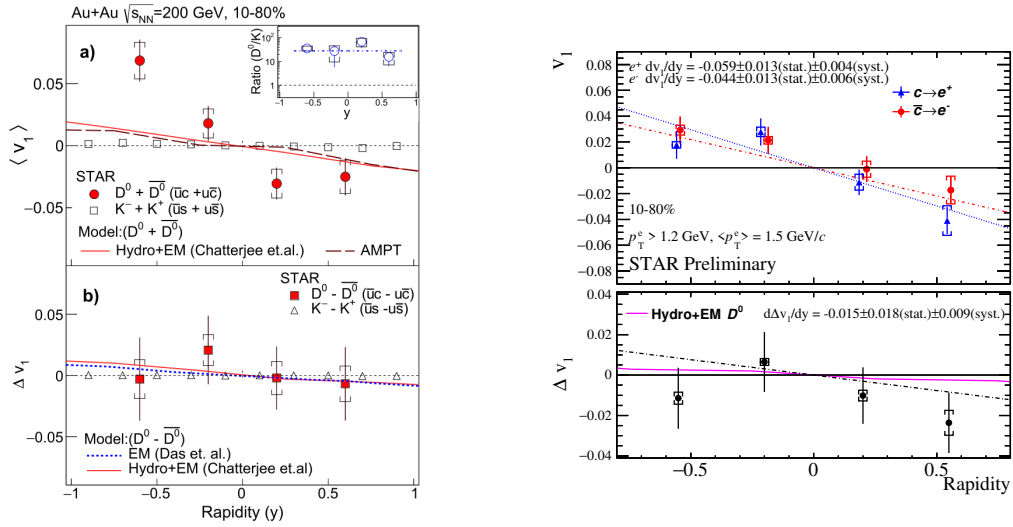


**Figure 5:** Directed flow  $v_1$  of  $D^0$  and  $\bar{D}^0$  at  $p_T > 1.5$  GeV/c compared to that of kaons at  $p_T > 0.2$  GeV/c [14] (left) and  $v_1$  of charm decayed positrons and anti-charm decayed electron at  $p_T > 1.2$  GeV/c as a function of rapidity in 10–80% central Au+Au collisions compared to model calculations (right).

## 107 Acknowledgments

108 The work was supported from European Regional Development Fund-Project "Center of Ad-  
 109 vanced Applied Science" No. CZ.02.1.01/0.0/0.0/16-019/0000778 and by the grant LTT18002 of  
 110 Ministry of Education, Youth and Sports of the Czech Republic.

## 111 References

- 112 [1] STAR collaboration, *Nucl. Phys. A* **757** (2005) 102.  
 113 [2] Z.-W. Lin and M. Gyulassy, *Phys. Rev. C* **51** (1995) 2177.  
 114 [3] STAR collaboration, *Nucl. Phys. A* **931** (2014) 1141.  
 115 [4] STAR collaboration, *Phys. Rev. C* **99** (2019) 034908.  
 116 [5] S. Cao, G.-Y. Qin and S.A. Bass, *Phys. Rev. C* **92** (2015) 024907.  
 117 [6] STAR collaboration, *Phys. Rev. Lett.* **124** (2020) 172301.  
 118 [7] S. Plumari, V. Minissale, S.K. Das et al., *Eur. Phys. J. C* **78** (2018) 348.  
 119 [8] ALICE collaboration, *Eur. Phys. J. C* **77** (2017) 550.  
 120 [9] ALICE collaboration, *JHEP* **10** (2018) 174.  
 121 [10] M. He, R.J. Fries and R. Rapp, *Phys. Rev. Lett.* **110** (2013) 112301.  
 122 [11] J. Zhao, S. Shi, N. Xu et al., 1805.10858.  
 123 [12] A.M. Poskanzer and S.A. Voloshin, *Phys. Rev. C* **58** (1998) 1671.  
 124 [13] STAR collaboration, *Phys. Rev. Lett.* **118** (2017) 212301.  
 125 [14] STAR collaboration, *Phys. Rev. Lett.* **123** (2019) 162301.